

PROCEEDINGS OF SPIE

[SPIDigitalLibrary.org/conference-proceedings-of-spie](https://spiedigitallibrary.org/conference-proceedings-of-spie)

Design and characterization of 1.1 micron pixel image sensor with high near infrared quantum efficiency

Zach M. Beiley
Andras Pattantyus-Abraham
Erin Hanelt
Bo Chen
Andrey Kuznetsov
Naveen Kolli
Edward H. Sargent

Design and characterization of 1.1 micron pixel image sensor with high near infrared quantum efficiency

Zach M. Beiley, Andras Pattantyus-Abraham, Erin Hanelt, Bo Chen, Andrey Kuznetsov, Naveen Kolli and Edward H. Sargent
InVisage Technologies, 7979 Gateway Blvd Suite 240, Newark, CA 94560

ABSTRACT

At the 940 nm wavelength, solar background irradiance is relatively low and device-mounted monochromatic LED emission can be used to illuminate and assess the shape, distance, and optical properties of objects. We report here NIR imaging that outperforms existing CMOS sensors by achieving record 42% quantum efficiency at 940 nm for a 1.1 μm pixel. The rationally engineered material properties of QuantumFilm allow tuning of the spectral response to the desired wavelength to achieve quantum efficiency that exceeds 40%. In addition, the combination of high QE with QuantumFilm's distinctive film-based electronic global shutter mechanism allows for extremely low illumination power and therefore lowers time-averaged system power when imaging with active illumination.

1. INTRODUCTION

High-resolution machine vision in a variety of environments is important for numerous applications. Human-machine interaction has evolved to new levels through eye tracking, gesture recognition and motion sensing, and autonomous vehicles are poised to revolutionize the transportation of goods and people. These applications require a high-resolution, high-sensitivity, low-cost and low-power image sensor operating at a wavelength where the background solar irradiance is low.

QuantumFilm's high NIR sensitivity and global shutter capability are particularly useful for active illumination imaging systems, including structured light. These devices rely on highly accurate detection of variations to a specific pattern of invisible NIR illumination as it is reflected back to the sensor for applications such as collision avoidance, range sensing, and 3-D mapping.

In the 940 nm window, QuantumFilm-enabled image sensors compete with conventional silicon-based sensors, which can have 4 and 5 transistors per pixel (4T and 5T, respectively). Table 1 compares the properties of these image sensors for effective 940 nm imaging. **Resolution** is determined both by pixel pitch and modulation transfer function (MTF). **High sensitivity** is quantified by the external quantum efficiency (QE), which is the product of optical absorption efficiency (OE) and internal quantum efficiency (IQE), and should be as close to 100% as possible. **Dynamic scene imaging** is enabled by the presence of global shutter functionality in each pixel. Only the QuantumFilm platform simultaneously meets all three criteria.

Table 1. Comparison of image sensors for 940 nm imaging

Imaging Goal	Requirement	Silicon 4T Image Sensors	Silicon 5T Image Sensors	Spark4K with QuantumFilm
High resolution	Small pixel ($\leq 1.1 \mu\text{m}$) and high MTF	Yes	No	Yes
High sensitivity to 940 nm light	High absorption coefficient at 940 nm	No	No	Yes
Dynamic scene imaging	Global shutter	No	Yes	Yes

We describe herein the design of the optical stack of the QuantumFilm image sensor, which allowed it to exceed 40% QE at 940 nm. We also compare QuantumFilm device performance with that of conventional silicon sensors, and outline a roadmap for further advances in performance.

2. QUANTUMFILM DEVICE

The QuantumFilm stack is shown in Figure 1 and has been described previously¹. It consists of multiple layers of semiconducting, insulating and metallic materials, such that incident photons are efficiently absorbed and converted to charges, which are extracted to the electrodes. Each pixel in the image sensor is defined by the patterned bottom electrode, which is connected to the underlying silicon-based read-out circuits.

Incident light is focused via infrared-optimized microlenses through the anti-reflection (AR) layer to reach the photoactive layer, where it is absorbed by semiconductor quantum dots and converted into holes and electrons. The applied bias between the top and bottom electrodes causes one charged species to be collected at the bottom electrode. This applied bias also allows global shutter operation, which is described in detail elsewhere².

3. OPTIMIZATION OF THE OPTICAL STACK

The QuantumFilm stack is designed to absorb as large a fraction of the incident 940 nm light as possible. Light that is not absorbed is lost either to reflection or transmission, so the design must correspondingly maximize absorption while minimizing reflection and transmission.

The properties of each layer in the stack have an effect on the optical behavior. In this work, the substrate and electrode properties and thicknesses were kept fixed, and the following parameters were chosen for optimization: thickness of the dielectric AR layer, use of microlenses, and thickness and absorption coefficient of QuantumFilm.

To obtain an accurate understanding of absorption, scattering and diffraction at the pixel level, a Finite Difference Time Domain (FDTD) model was used (Lumerical Solutions, Inc.). The model consisted of a 6×6 pixel structure, with the simulation region comprising a 2×2 pixel block in the center. Material properties for each layer were either measured by ellipsometry or taken from the Lumerical materials database.

The boundary conditions were periodic in the x and y-direction. Perfectly matched layer absorbing boundary conditions were used in the z-direction. A conformal mesh with at least 10 cells per wavelength was used to accurately calculate the fields throughout the model. The illumination source was a plane wave centered at a wavelength of 940 nm. The source was located above the top layer of the sensor stack and propagated down into the stack. The absorption in the QuantumFilm layer was calculated from the difference in transmission of light through the power monitors above and below the absorbing layer, normalized to the source power.

Figure 2 shows the effect of QuantumFilm and AR layer thickness on light absorption, with and without microlenses. Without microlenses, the maximum absorption in the QuantumFilm layer is 37%; with the aid of microlenses, it exceeds 42%. The microlenses also achieve this peak absorption with ~15% thinner QuantumFilm, which reduces both materials usage and thermally generated dark current.

Figure 3 shows the top surface reflection losses with and without microlenses. Both configurations are capable of reducing reflection losses below 2%, which indicates that the majority of optical losses are due to transmission into the substrate. For a fixed QuantumFilm absorption coefficient, the advantage of the microlens is that it focuses the light onto the bottom electrode, such that transmission losses are reduced and absorption increased, as confirmed by the field intensity plot in the vertical plane of the pixel (Figure 4).

4. OPTIMIZATION OF QUANTUMFILM PROPERTIES

QuantumFilm thickness and absorption coefficient play a dominant role in determining the total absorption. Table 2 compares the absorption coefficient of QuantumFilm and silicon at 940 nm: QuantumFilm's absorption exceeds that of silicon by a factor of more than 60. A higher absorption coefficient is the key enabler of high sensitivity in small pixels, and the QE increase from our previous report¹ was achieved by engineering a higher absorption coefficient.

The effect of increasing the absorption coefficient can be readily simulated by FDTD without re-optimizing the complete optical stack. As shown in Figure 5, the fraction of light absorbed increases with the absorption coefficient in the 5000 to 10000 cm⁻¹ regime, and agrees well with experimentally measured QE values. The fraction absorbed is also substantially

greater than the single pass limit, indicating that multi-pass absorption is occurring due to reflection from the bottom electrode and substrate.

Table 2. Comparison of the absorption coefficient for QuantumFilm vs silicon in the near infrared (940 nm).

Material	Absorption Coefficient at 940 nm (cm ⁻¹)	Quantum Efficiency at 940nm (%) [*]
Silicon ^[2]	130	~7
QuantumFilm ^[1]	5300	35
QuantumFilm - This work	8400	42

^{*}1.1 μm pixel image sensors

5. APPLICATION PERFORMANCE

4.1 Enhanced Sensitivity

The QE spectrum of a Spark4K image sensor is shown in Figure 6 in relation to the solar spectrum. QuantumFilm’s QE advantage at 940 nm can be visualized directly with images taken at identical integration times and fixed illumination pulse durations. An Invisage Spark4K sensor (13 megapixels, 1.1 μm pixel size) with QuantumFilm is compared with an off-the-shelf BSI silicon-based image sensor (13M pixels, 1.1 μm pixel size) Figure 7. The images taken with QuantumFilm are brighter and allow for better identification of scene objects. It is notable also that the 940 nm illumination sees through the lenses of the sunglasses in the foreground of the image—a valuable capability for security and iris recognition.

4.2 Enhanced Resolution with Global Shutter

A silicon-based image sensor pixel is typically at-least 3 μm in size to accommodate the transistors needed for global shutter operation. In contrast, the QuantumFilm pixel can implement a film-based global shutter with a 1.1 μm pixel, enabling a dramatic increase in resolution previously unachievable in infrared imaging. This resolution increase is quantified in the modulation transfer function, as shown in Figure 8, at both visible (530 nm) and near infrared (940 nm) wavelengths. An advantage evident from the figure, is that the thin QuantumFilm layer utilized for high sensitivity in NIR, has very low crosstalk even at longer wavelengths making exceptionally high MTF possible. A silicon-based NIR image sensor with a typical 3 μm pixel pitch cannot achieve the MTF performance of QuantumFilm even in an ideal scenario, and will incur increased crosstalk due to the thickening of Silicon necessary for even moderate levels of absorption in NIR.

6. QUANTUM EFFICIENCY ROADMAP

The current record quantum efficiency can be improved further to be much closer to the theoretical limit of 100%. Since quantum efficiency is presently limited by the amount of light absorbed in the QuantumFilm, gains in 940 nm response will be achieved by tuning the film thickness, the absorption coefficient at 940 nm and interface reflections.

7. CONCLUSIONS

We have demonstrated a record QE exceeding 42% at 940 nm for 1.1 μm pixel image sensors, using an optimized optical stack incorporating QuantumFilm. This was achieved through combined optimization of absorption coefficient, reflection losses and transmission losses. We demonstrate that QuantumFilm sensor MTF is superior to conventional silicon sensors. Higher sensitivity to NIR wavelengths enables higher resolution, and in combination with QuantumFilm’s global shutter, makes QuantumFilm technology beneficial for any NIR imaging application requiring fine and long-range detection of detail, active illumination including structured light, and effective NIR imaging performance outdoors.

8. REFERENCES

- [1] Mandelli, E.; Beiley, Z.M.; Kolli, N.; Pattantyus-Abraham, A.G., "Quantum dot-based image sensors for cutting-edge commercial multispectral cameras," Proc. SPIE 9933, Optical Sensing, Imaging, and Photon Counting: Nanostructured Devices and Applications 2016, 993304 (2016)
- [2] Green, M.A. and Keevers, M. J., "Optical properties of intrinsic silicon at 300 K," Prog. Photovolt: Res. Appl., 189 (1995).
- [3] Beiley, Z.M.; Cheung, R.; Hanelt, E.; Mandelli, E.; Meitzner, J.; Park, J.; Pattantyus-Abraham, A.G.; Sargent, E.H., "Device design for global shutter operation in a 1.1 μm pixel image sensor and its application to near infrared sensing," Proc. SPIE 10098, Physics and Simulation of Optoelectronic Devices XXV, submitted (2017)

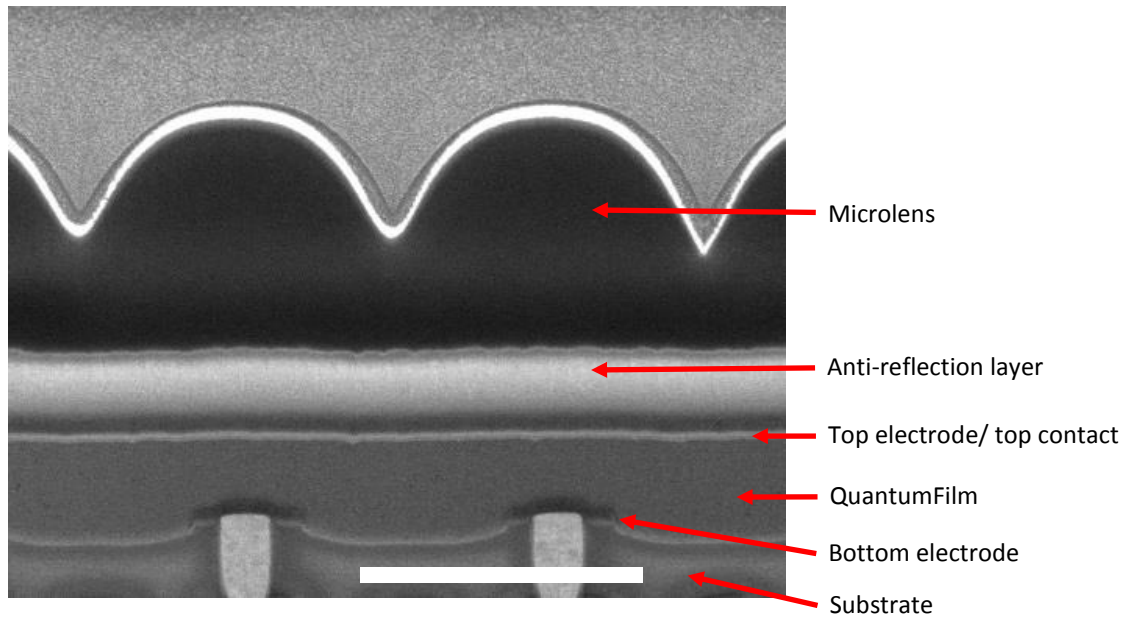


Figure 1. Scanning electron microscope cross-section of the QuantumFilm stack with 1.1 μm pixels (tilt view). The scale bar is 1 μm .

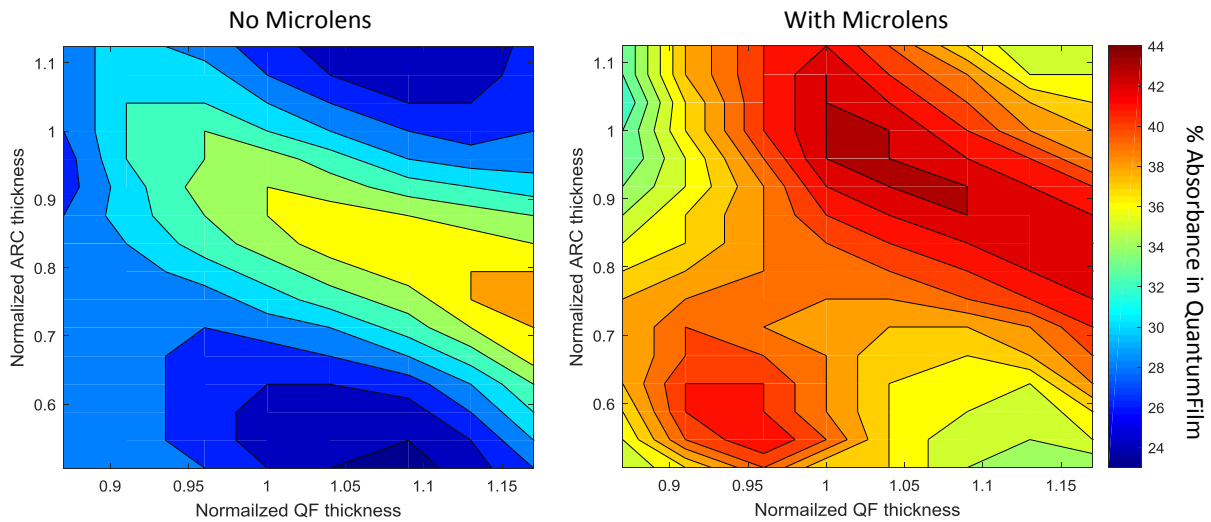


Figure 2. Contour plots of 940 nm absorbance showing the combined optimization of QuantumFilm and AR layer thickness, with and without microlenses on each pixel.

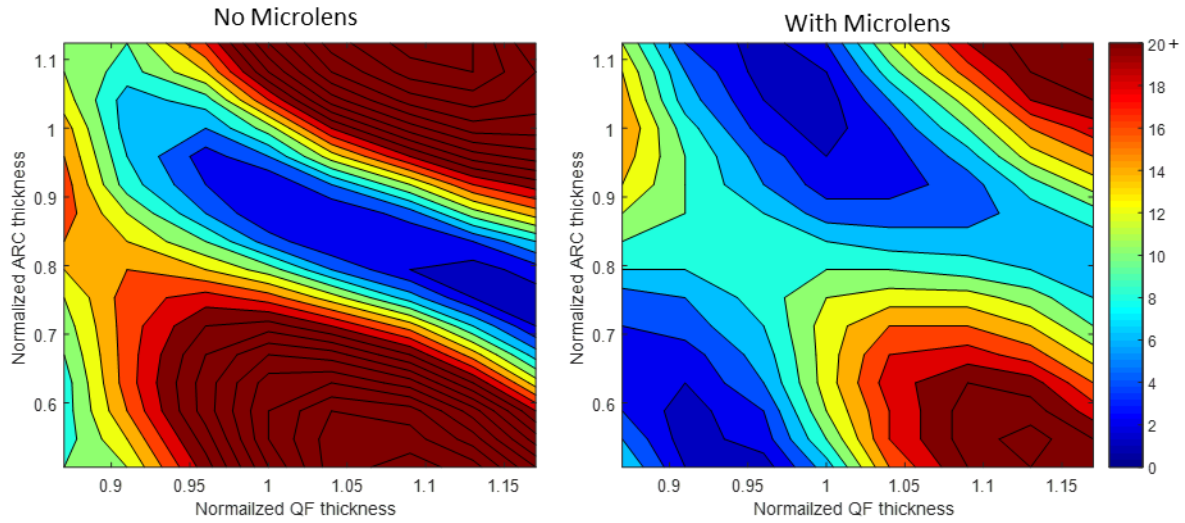


Figure 3. Contour plots of top surface reflection at 940 nm from the QuantumFilm stack (a) with AR layer and (b) with AR layer and microlens.

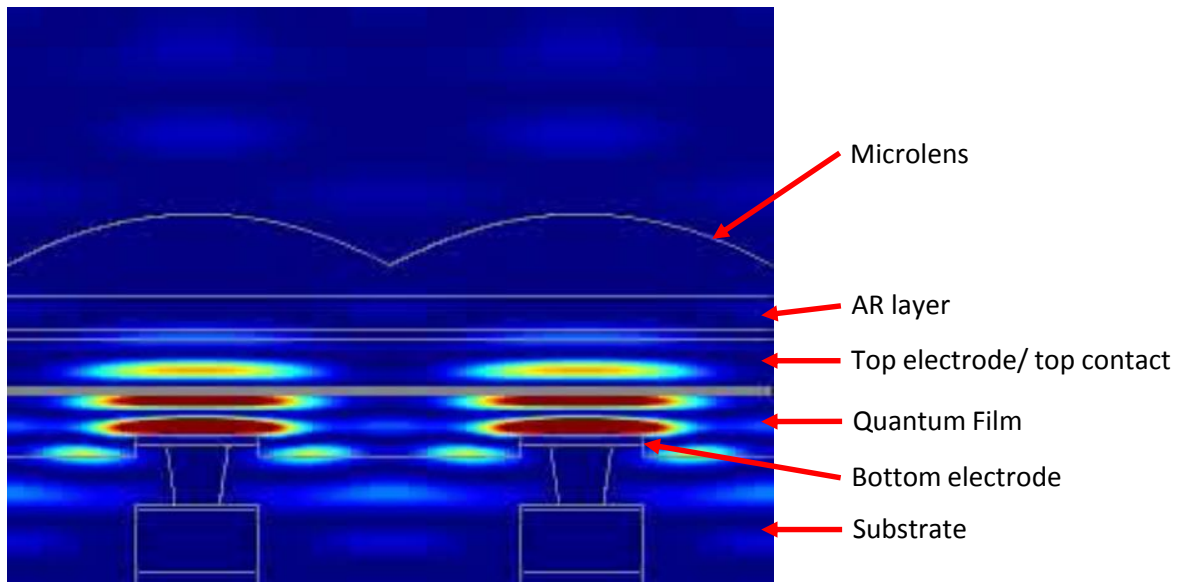


Figure 4. Simulated optical field intensity ($|E|^2$) from 940 nm illumination on QuantumFilm stack over two pixels with AR layer and microlens.

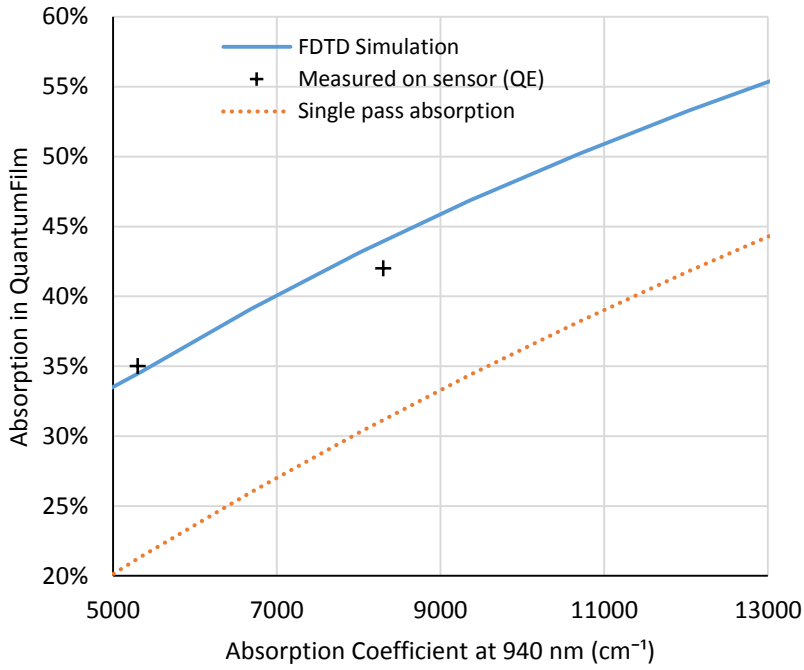


Figure 5. Effect of absorption coefficient on fraction of light absorbed in QuantumFilm, compared with experimentally measured QE.

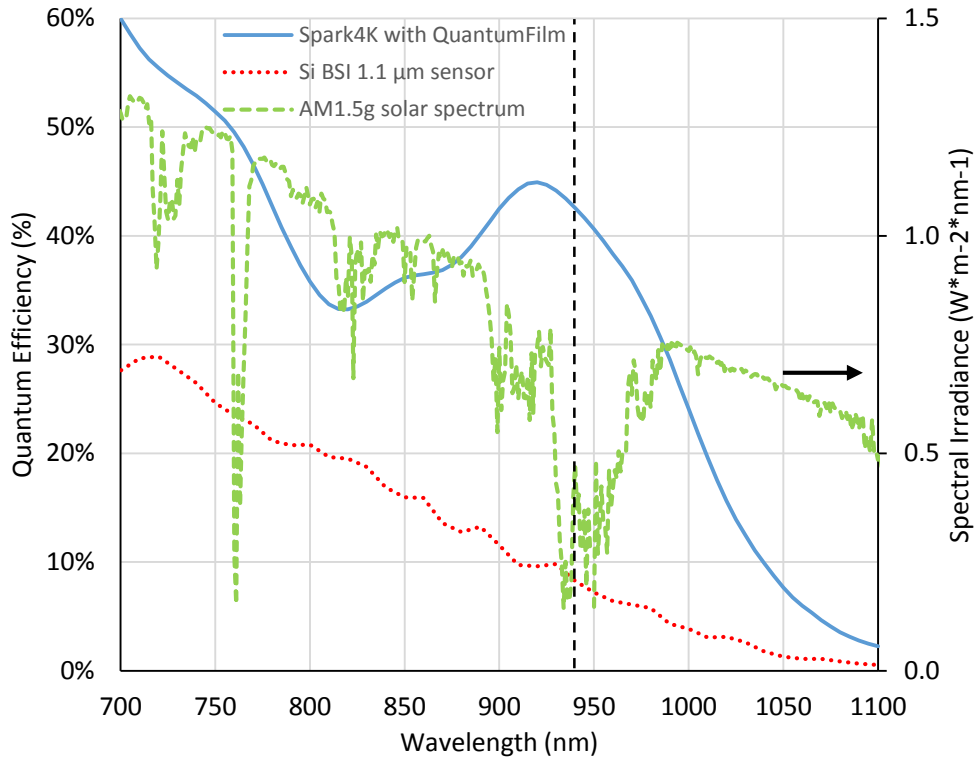


Figure 6. Comparison of quantum efficiency spectra of Spark4K with QuantumFilm and 1.1 μm pixel silicon-based BSI sensor.



Figure 7. Comparison images taken with Spark4K with QuantumFilm and a silicon-based 13-megapixel (1.1 μm pixel size) image sensor. The 940 nm LED pulse durations were 10 ms in both cases.

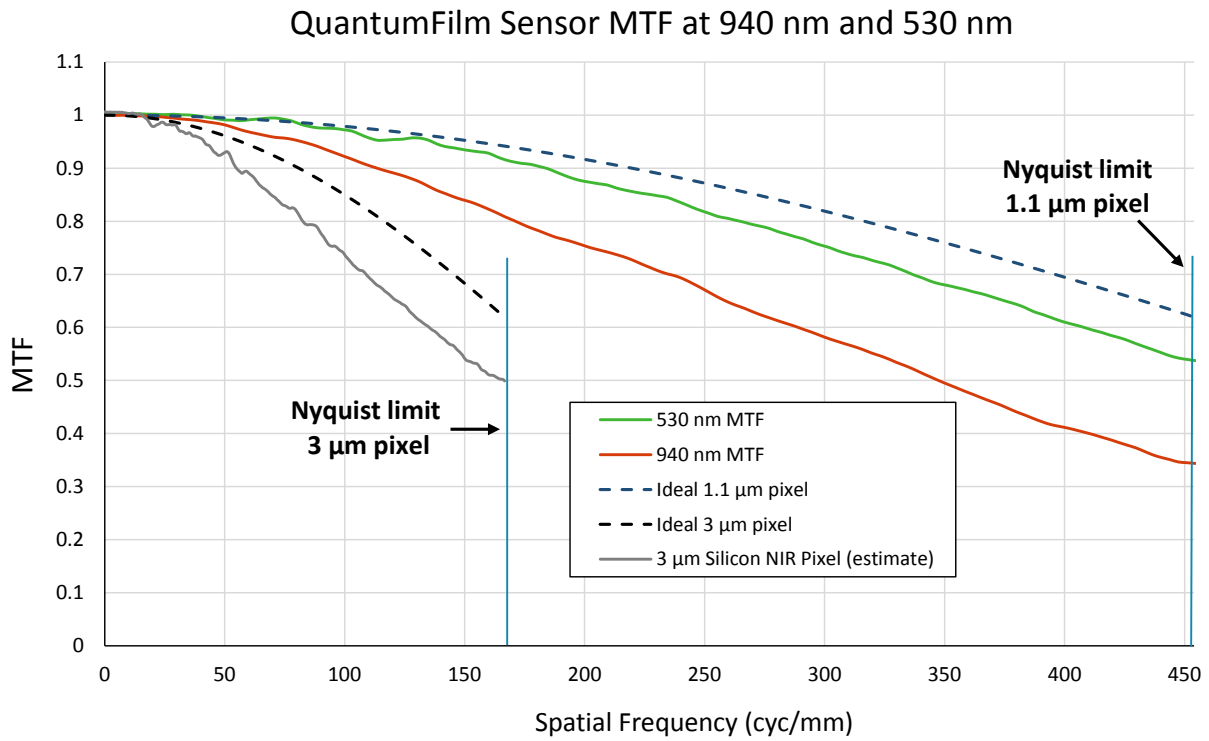


Figure 8. Modulation transfer function (MTF) comparison of Spark4K with QuantumFilm (1.1 μm) and a silicon-based sensor (estimate based on 3 μm pixel).